



Statistical physics of active processes in cells

Frank Jülicher

Max-Planck-Institut für Physik komplexer Systeme, Nöthnitzer Str. 38, 01187 Dresden, Germany

Available online 2 May 2006

Abstract

Simple concepts from statistical physics are discussed to describe the transduction of chemical energy of a fuel to mechanical work on the molecular level. Such approaches can characterize general physical features of motor proteins that generate forces in the cell cytoskeleton. In integrated cellular systems such as cilia and hair bundles, cytoskeletal filaments and motors form complex structures and interact in large numbers. In such systems the interplay of filaments and motors can lead to emergent dynamic behaviors such as oscillating collective modes or to wave-like patterns. We discuss general aspects of such dynamic states and relate them to the dynamics of cytoskeletal structures in cells.

© 2006 Elsevier B.V. All rights reserved.

1. Introduction

One of the most striking features of life and living cells is their ability to move and exhibit active behaviors. Cells are extraordinarily dynamic and are able to generate motion and forces [1,2]. Prominent examples for dynamic processes in cells are cell motility, muscle contraction and active processes that take place inside cells such as cell division and material and organelle transport in the cell. Other examples involve proteins that move along DNA in order to copy, read or repair the information stored in the base pair sequence. Motion and forces are generated on the molecular level by protein molecules that use the hydrolysis of a fuel, typically of adenosinetriphosphate (ATP), as energy source. Typical examples are highly specialized motor proteins which operate in all eucaryotic cells. Eucaryotic cells possess a nucleus and include the cells of all higher organisms (animals and plants) and some single celled organisms. These cells possess a cytoskeleton which is a complex three-dimensional network of rod-like filaments which are built of proteins subunits [2]. This filament network provides the cell with mechanical stability and integrity and can be viewed as a viscoelastic gel-like material.

The cytoskeleton is a prototype system for the study of force and motion generation in cells. The dynamical properties of the cytoskeleton and its associated proteins are governed by phenomena on different scales. On the molecular level, motor proteins transduce chemical energy of ATP hydrolysis to generate motion and forces [3–5]. These forces are stochastic in nature. On larger scales, the cytoskeleton forms complex structures and dynamical behaviors emerge from an interplay of many active processes. Certain types of such behaviors can be described as arising via self-organization phenomena. This can be illustrated by focussing on simple

E-mail address: julicher@mpipks-dresden.mpg.de.

URL: <http://www.mpipks-dresden.mpg.de/mpi-doc/julichergruppe/julicher/index.html>.

examples, where complex patterns in space and time can be understood to be generated by molecular motors interacting with cytoskeletal filaments [6–8].

A large number of active elements such as motors working together in groups can give rise to new types of mechanical behaviors. In general, dynamic instabilities and bifurcations can occur in this case via collective effects. A simple situation where the self-organization of motors and filaments occurs are bundles of filaments in the presence of motors and cross-linkers. Such bundles occur in cells as the so-called stress fibers or they form a contractile ring to constrict a dividing cell. Theoretical analysis shows that such bundle can exhibit active properties if motor molecules or aggregates of motors form mobile cross-linkers [9–11]. These motors slide filament pairs with respect to each other which introduces a rich dynamics in the system and active mechanical properties. With the presence of motors, the passive filament bundle has been transformed in a nonlinear dynamic system. In this system, dynamic patterns and complex mechanical properties can occur. Filaments can be cross-linked and form gel-like materials with viscoelastic properties. In the presence of motor-aggregates, these gels become active and exhibit new material properties [12,13].

Collective behaviors of many active elements can also lead to the generation of mechanical oscillations [14,15]. Motor-induced mechanical oscillations of cells occur in a number of different situations. Oscillatory motion is important for the periodic beating of cilia and flagella which some microorganisms use to swim [1]. These cilia are elastic hair-like appendages which move periodically and generate wave-like bending patterns which are used for swimming and propulsion. Here, oscillations have been suggested to result from the self-organization of many motor proteins which induce the bending of elastic filaments in the cilia [16]. Oscillations can also result as unavoidable side effect of the underlying dynamics in a cell. An example is cell divisions which are asymmetric. In this case, oscillations of the mitotic spindle are observed. The spindle is built of cytoskeletal filaments and plays the role to physically separate the duplicated chromosomes. It is a dynamic structure, stabilized by motor proteins. It has been shown that the interplay of many motors at the outer cell membrane which exert forces on the mitotic spindle undergo an oscillating instability as the number of active motors is increased by the cell [15].

Mechanical oscillations also play a role for the detection of mechanical stimuli by mechanosensory cells [17,18]. Mechanosensory cells of the ears of vertebrates exhibit complex cytoskeletal structures which form bundles of rod-like stereocilia [19]. These hair bundles have been shown to generate spontaneous mechanical oscillations [20,21] which result from the interplay of motor proteins, ion channels and a feedback regulation of motor forces by Ca-ions [21,22].

In the subsequent sections, we discuss approaches of physics to describe general features of active phenomena in cells. Starting with the statistical physics of motor proteins, we discuss how complex dynamic behaviors emerge via collective effects in groups of cooperating motors and more complex cellular structures.

2. Motors of the cytoskeleton

A motor protein of the cytoskeleton interacts specifically with a certain type of filament along which it moves in presence of ATP [3]. The filaments serve as guides or tracks for the motion. Two types of filaments play this role: microtubules and actin filaments. Both are formed by a polymerization process from identical monomers (actin and tubulin monomers, respectively), leading to a regular and periodic structure. An important feature is their structural polarity: the filaments are asymmetric with respect to their two ends. This symmetry has its origin in the asymmetry of the monomers which polymerize in a regular periodic structure to form a polar filament. The two different ends of the filament are denoted as “plus end” and “minus end”. This polar symmetry is essential for motor operation as it defines the direction of motion. A given motor molecule moves in a particular direction along a filament. Motor proteins are classified into several families: myosins, kinesins and dyneins. Myosins move always along actin filaments while kinesins and dyneins move along microtubules, see Fig. 1.

The motor protein (or more precisely, the head domain containing the ATP-binding site) undergoes a chemical cycle. It binds ATP, hydrolyzes the bound ATP and releases the products of the hydrolysis reaction ADP and P (phosphate). After completion of the cycle the motor is unchanged. The different conformations

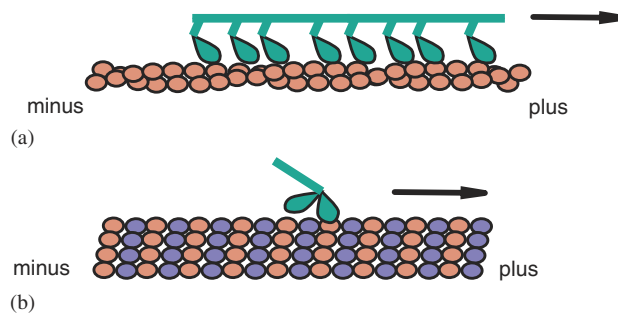


Fig. 1. Schematic representation of molecular motors and track filaments. (a) Myosin molecules often interacting in large groups with an actin filament. (b) Kinesin with two identical “heads” moving along a microtubule. Actin filaments and microtubules exhibit structural polarity and result from periodic arrangements of monomers. Their two different ends are denoted as “plus” and “minus”.

which occur during the chemical cycle have different structural conformations and can in particular have different interaction characteristics with respect to the filament. As a result, the motor protein periodically undergoes chemistry-driven changes between different conformations. This coupling between chemistry and binding permits the creation of motion along a polar filament [3–5,23–27].

3. Isothermal ratchets

How can directed motion be generated from a chemical reaction? First, let us state very general requirements. Motion can occur if two separate symmetries are broken. (i) The filaments must be polar and distinguish motion in opposite directions. (ii) Invariance with respect to time reversal must be broken. This implies an irreversible or nonequilibrium process. If either of the two symmetries is present, on average no motion can possibly occur. Any displacement that is generated can in this case be undone by an equally likely process acting in the opposite direction.

For motor proteins both symmetries are broken and directed motion is expected to occur. However, in order to characterize the physics of motion generation, we need explicit models. Firstly, it is important to note that an irreversible situation cannot be achieved by temperature differences, since at the molecular scale temperature gradients relax on time scales much faster than the characteristic times of milliseconds for motor molecules. Since the filaments provide periodic sets of binding sites and considering their polar structure, it is convenient to think of these systems as generalized ratchets which rectify the chemical reaction to generate directed motion under isothermal conditions.

A simple physical representation of such an isothermal ratchet can be formulated as follows [4,5,28–30]: if we consider a motor in conformation i , we can define a potential or interaction energy profile along the filament. Suppose that one small region of the motor, e.g. in the tail, is used to transmit forces or to attach a cargo. We imagine this point to be held at a position x along the filament. We can now define $W_i(x)$ to be the energy of the motor, including possibly bound ATP, ADP or P, and including the energy of the filament as the motor is held at position x . This total energy is in fact an effective free energy defined formally by integrating over all rapidly relaxing microscopic degrees of freedom but keeping the enzyme in its chemical state. The conformation of the system motor-filament is then fully characterized by the pair $\{i, x\}$ of internal state and position with respect to the filament, where $i = 1, \dots, m$ and m is the number of states. Note that the potentials reflect the symmetry properties of the filament. If the filament is polar and a periodic array of identical monomers, the potentials are periodic with period l , $W_i(x) = W_i(x + l)$ and asymmetric, $W_i(x) \neq W_i(-x)$.

In order to describe the dynamics of the system $\{i, x\}(t)$, we use a stochastic overdamped dynamics at constant temperature T within a given state i

$$\eta_i \frac{d}{dt} x = -\partial_x W_i(x) + \zeta_i(t). \quad (1)$$

Here, η_i is a protein friction and $\zeta(t)$ is a Gaussian white noise in state i with $\langle \zeta_i(t)\zeta_j(0) \rangle = 2\eta_i\delta(t)$. The chemical reactions between states $\{i, x\}$ and $\{j, x\}$



occur with Poisson statistics with reaction rates $\omega_{ij}(x)$. Since the position variable x is also a conformational degree of freedom (the motor, in general, changes its shape while displacing), transition rates are, in general, x -dependent. Note that for simplicity in Eq. (2) we have assumed that transitions between states happen instantaneously and without displacement. Furthermore, we have used the fact that thermal relaxation is very fast compared to the chemical cycle and all rapid degrees of freedom are equilibrated at constant temperature T . In fact, the typical relaxation time of temperature gradients which have developed on a length scale l can be estimated as $\tau = Cl^2/\kappa$, where C is the specific heat of the material per volume and κ the thermal conductivity. Using typical values for water and length scales of the order of 10 nm we find $\tau \simeq 10^{-6} - 10^{-8}$ s, which is fast compared to typical cycle times of several ms. This argument shows that the motor operates isothermally, i.e., temperature gradients are not created and cannot be used to generate motion as e.g. in the case of Feynman's ratchet [31].

It is now convenient to use a description based on probability distributions and to introduce distribution functions $P_i(x, t)$ for the probability to find within an ensemble of identical systems the motor at time t at position x in state i . These distributions then obey the equations

$$\partial_t P_i + \partial_x J_i = \sum_{j \neq i} (\omega_{ji}(x)P_j(x) - \omega_{ij}(x)P_i(x)), \quad (3)$$

$$J_i = \eta_i^{-1}(-k_B T \partial_x P_i - P_i \partial_x W_i + P_i f_{ext}) \quad (4)$$

which are Smoluchowsky equations [32] with source and sink terms. The total density and total current

$$P(x, t) = \sum_{i=1}^m P_i, \quad (5)$$

$$J(x, t) = \sum_{i=1}^m J_i \quad (6)$$

obey the conservation law $\partial_t P + \partial_x J = 0$. The average velocity in the steady state with stationary and periodic distribution function $P_i(x) = P_i(x + l)$, $\partial_t P_i = 0$ is given by

$$v = \int_0^l J dx / \int_0^l P dx. \quad (7)$$

In order to characterize the chemical rates, we first introduce the chemical potentials of the fuel and hydrolysis products in bulk solution. We denote μ_{ATP} , μ_{ADP} and μ_P the free energy per ATP, ADP or P molecule, respectively. As an illustrative example, we first consider the four chemical states ($m = 4$): the motor M ($i = 1$), M-ATP ($i = 2$), M-ADP-P ($i = 3$) and M-ADP ($i = 4$), often encountered for biological motor proteins. A general reaction kinetics for all eight reaction rates which is consistent with the ATP hydrolysis reaction can be written as

$$\begin{aligned} \omega_{12} &= \alpha_1 \exp[(W_1 + \mu_{ATP})/k_B T] & \omega_{21} &= \alpha_1 \exp[W_2/k_B T], \\ \omega_{23} &= \alpha_2 \exp[W_2/k_B T] & \omega_{32} &= \alpha_2 \exp[W_3/k_B T], \\ \omega_{34} &= \alpha_3 \exp[W_3/k_B T] & \omega_{43} &= \alpha_3 \exp[(W_4 + \mu_P)/k_B T], \\ \omega_{41} &= \alpha_4 \exp[(W_4 + \mu_P)/k_B T] & \omega_{14} &= \alpha_4 \exp[(W_1 + \mu_{ADP} + \mu_P)/k_B T]. \end{aligned} \quad (8)$$

Here, we have used the condition of detailed balance of the rates. The functions $\alpha_i(x)$ characterize the kinetic rates of the reactions. Note that since transitions are fast and therefore occur for fixed x , the chemical rates do not depend on the external force f_{ext} or local stresses. Only displacements described by Eq. (1) are force-dependent. The present modelization differs in this respect from models which use discrete transitions also to

describe displacements. In this case chemical rates are strain-dependent [25,33–36]. From a physical point of view, all models are of course equivalent.

It is useful to further simplify the generic description introduced above. The m -state model allows in principle to describe many details of the chemical cycle and the various conformations of the motor. However, it contains a large number of free parameters which are unknown. In order to describe physical aspects of motion generation and force generation, it is sufficient to keep only two different states ($m = 2$) [27–29,37].

We rewrite the Fokker–Planck equations (4) for two states $i = 1, 2$:

$$\partial_t P_1 + \partial_x J_1 = -\omega_1(x)P_1 + \omega_2(x)P_2,$$

$$\partial_t P_2 + \partial_x J_2 = \omega_1(x)P_1 - \omega_2(x)P_2, \tag{9}$$

where we have introduced $\omega_1 = \omega_{12}$ and $\omega_2 = \omega_{21}$ and the currents are the same as introduced in Eq. (4). This system is sketched in Fig. 2 for an example of shifted periodic and asymmetric potentials.

This two-state model is still very flexible and allows to describe situations which capture many of the physical aspects of biological protein motors. Fig. 3 shows choice of potentials W_1 and W_2 adapted to the classical picture of myosin II function [26]: a myosin head detaches from the actin filament after binding ATP. In the unbound state ATP is hydrolyzed ($M-ATP \rightarrow M-ADP-P$). The head ($M-ADP-P$) is now again able to bind actin. As it encounters a binding site along the filament, it re-attaches under phosphate release. After re-attachment, a force-generating step occurs and ADP is released, which completes the chemical cycle. As

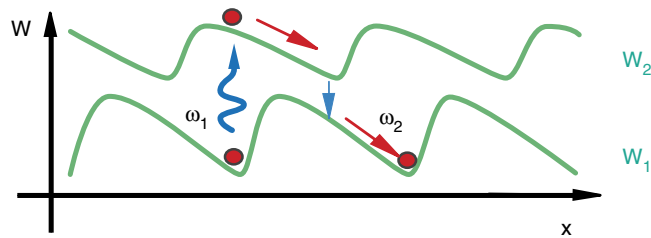


Fig. 2. Two-state model defined by two polar and periodic potentials W_1 and W_2 as well as periodic transition rates ω_1 and ω_2 . Pumping between the two states induces average motion.

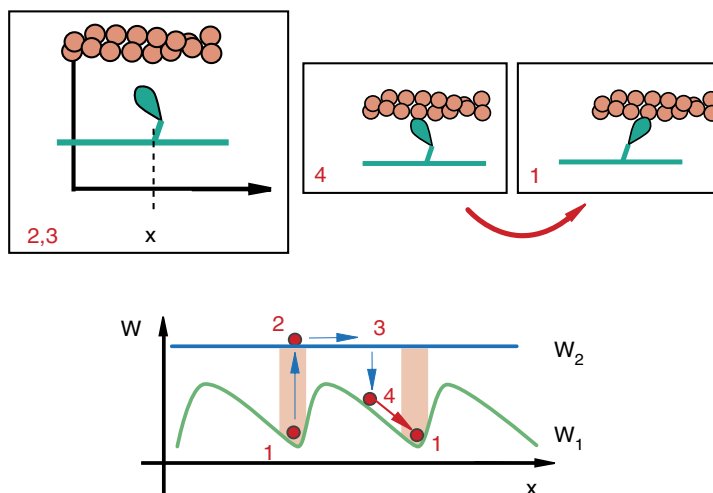


Fig. 3. Two-state model representing a situation motivated by nonprocessive motors such as myosin II. (1) Binding an ATP molecule, the motor detaches from the filament (2). After hydrolysis (3), it rebinds and generates a force (4) and a displacement. In a two-state model, two potentials W_1 and W_2 characterize attached and detached states with the tail at position x . The shaded areas are “active sites” where ATP-driven transitions occur.

illustrated in Fig. 3 this process can be captured by two different potentials, W_1 and W_2 representing the unbound state (a flat potential) and the bound state (a potential with periodic structure), respectively. After the force-generating step (power-stroke), the x variable has reached a potential minimum. Here, the system can be actively excited to the unbound state under ATP-binding. As it re-attaches to the filament, the slope of the potential reflects the mechanical force generated at this point. A displacement is generated as the system slides downhill along the energy profile to reach the potential minimum. Note that microscopically this displacement could correspond either to a tilt of the head domain as sketched in the figure or to other more complex processes. The microscopic structure associated with this displacement is not characterized by this description.

In a two-state picture, the chemical reaction cycle as described by the kinetic equations (8) has to be divided into two substeps. One possibility is to introduce the forward and backward rates α_1 and α_2 for the combined process of ATP-binding and hydrolysis



and the rates β_1 and β_2 which describe the process of product release and binding:



The complete chemical cycle is now the subsequent transitions α_1 and β_2 . As long as α_2 and β_1 are nonzero, there is a nonvanishing probability for an inversion of the cycle (i.e., ATP generation) by following the steps α_2 and β_1 . We define W_1 to be the energy of a free motor together with the product molecules ($M + \text{ADP} + \text{P}$) and W_2 to be the energy of the complex $M\text{-ADP-P}$. Detailed balance of the chemical reactions then implies

$$\frac{\alpha_1}{\alpha_2} = e^{(W_1 - W_2 + \Delta\mu)/k_B T}, \quad (12)$$

$$\frac{\beta_1}{\beta_2} = e^{(W_1 - W_2)/k_B T}, \quad (13)$$

where we have introduced the chemical driving force

$$\Delta\mu \equiv \mu_{\text{ATP}} - \mu_{\text{ADP}} - \mu_{\text{P}}. \quad (14)$$

The transition rates of the two-state model are the superpositions $\omega_i = \alpha_i + \beta_i$. Introducing two unknown functions $\alpha(x)$ and $\beta(x)$ which describe conformation-dependent energy barriers, we can therefore write

$$\begin{aligned} \omega_1(x) &= \alpha(x)e^{(W_1 + \Delta\mu)/k_B T} + \beta(x)e^{W_1/k_B T}, \\ \omega_2(x) &= [\alpha(x) + \beta(x)]e^{W_2/k_B T}. \end{aligned} \quad (15)$$

Note that other choices to divide the reaction cycle in two relevant substeps leads to the same result, but redefines the arbitrary functions α and β and shifts the potential W_2 by a constant value.

The functions $\alpha(x)$ and $\beta(x)$ define the coupling of the chemical reaction to conformation. Very important is the concept of localized or conformation-dependent transitions where the functions are peaked within a narrow x -interval but negligible outside this interval. An example is the ATP-binding step which in Fig. 3 is restricted to occur within an “active region” of conformation space corresponding to the potential minimum while the conformations at the beginning of a force-generating power stroke are not supposed to bind ATP. As we will describe in the subsequent sections, the localization of transitions via the functions α and β plays an important role for many interesting cases.

Similar to the case of myosin, the two-state model can also be adapted to other situations such as the motion of conventional kinesin molecules which are homodimers consisting of two identical heads both of which contain an ATP-binding site. In principle, a general description would require at least eight internal states and a complex reaction scenario. A possible simplification arises from the idea of a coordinated binding and unbinding of the two heads in a hand-over-hand fashion as shown schematically in Fig. 4 [38]. Such a coupling would reduce the number of relevant degrees of freedom [27]. In a two-state model, this feature can be

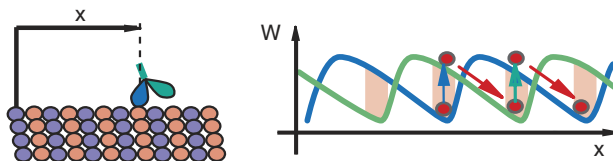


Fig. 4. Hand-over-hand motion suggested for double-headed conventional kinesins. At any time, one head is bound and the second head moves towards the next binding site. This situation can be represented by describing both heads by identical but shifted energy landscapes $W_1(x)$ and $W_2(x)$.

captured in a simplified way by associating each state with one of the heads being bound to the filament. Denoting the motor with head 1 or head 2 bound to the filament by M_1 and M_2 , respectively, we define the energies of these situations \bar{W}_1 and \bar{W}_2 . Because the two heads forming a kinesin motor are identical, the energy landscapes of both states are two identical potential profiles which are shifted with respect to each other by one monomer period $l/2$ on the filament: $\bar{W}_1(x) = \bar{W}_1(x + l)$; $\bar{W}_2(x) = \bar{W}_1(x + l/2)$, see Fig. 4. However, the characteristic step-size of an individual head l in this picture corresponds to two monomer sizes. Therefore, the potentials \bar{W}_i are l -periodic, while the total system is invariant under $x \rightarrow x + l/2$ if at the same time the two states are exchanged. Therefore, the transition rates also obey $\omega_1(x) = \omega_1(x + l)$ and $\omega_2(x) = \omega_1(x + l/2)$. Again, the idea of active regions and localized transitions is important. Assuming that all transitions occur at conformations which correspond to the potential minimum, we obtain a system which operates in an almost deterministic way where the chemical cycle is closely correlated to a particular displacement. In this case, forward stepping of the motor can for small external forces be tightly coupled to ATP hydrolysis events as is observed for conventional kinesins. In the case of nonlocalized transitions, the chemical cycle is related to motion in a more irregular way.

A useful representation of the transition rates in the hand-over-hand picture is to assume that a full ATP hydrolysis cycle changes M_1 to M_2 :



Because of the symmetry between the two heads, the reaction $M_2 + \text{ATP} \rightleftharpoons M_1 + \text{ADP} + \text{P}$ occurs with the same rates. This leads to the total transition rates

$$\begin{aligned} \omega_1(x) &= e^{\bar{W}_1(x)/k_B T} [\bar{\alpha}(x) e^{\bar{\Delta}\mu/k_B T} + \bar{\alpha}(x + l/2)], \\ \omega_2(x) &= e^{\bar{W}_2(x)/k_B T} [\bar{\alpha}(x) + \bar{\alpha}(x + l/2) e^{\bar{\Delta}\mu/k_B T}]. \end{aligned} \quad (17)$$

The unknown function $\bar{\alpha}(x) = \bar{\alpha}(x + l/2)$ is l -periodic. Note that the choice given in Eq. (17) is a special case of Eq. (15) if we identify $\Delta\mu = 2\bar{\Delta}\mu$, $\alpha(x) = \bar{\alpha}(x) e^{-\bar{\Delta}\mu/k_B T}$, $\beta(x) = \bar{\alpha}(x + l)$, $W_2 = \bar{W}_2 + \bar{\Delta}\mu$ and $W_1 = \bar{W}_1$. This example demonstrates that Eq. (15) is a general choice which can describe very different types of couplings of an ATP hydrolysis cycle to a two-state model.

4. Single motors

We will now discuss general properties of the two-state model for a single motor introduced above [28,39,40]. Two generalized forces act on the system leading to an out-of-equilibrium situation. These are the chemical “force” $\Delta\mu$ introduced in Eq. (14) and the mechanical force f_{ext} . If both generalized forces are kept constant, the system eventually attains a steady state with $\partial_t P_i = 0$. The steady state distribution functions satisfy two coupled differential equations of second order

$$\begin{aligned} k_B T \partial_x^2 P_1 + (\partial_x P_1)(\partial_x W_1 - f_{ext}) - P_1 \partial_x^2 W_1 &= \eta(\omega_1 P_1 - \omega_2 P_2), \\ k_B T \partial_x^2 P_2 + (\partial_x P_2)(\partial_x W_2 - f_{ext}) - P_2 \partial_x^2 W_2 &= -\eta(\omega_1 P_1 - \omega_2 P_2), \end{aligned} \quad (18)$$

where we have for simplicity assumed that the friction η is the same for both states. This set of equations together with periodic boundary conditions $P_i(x) = P_i(x + l)$ defines the steady state distributions. They can

be calculated in special cases analytically, but, in general, numerical integration techniques are used. For each pair $(\Delta\mu, f_{ext})$, there is a uniquely defined average velocity

$$v = \frac{1}{\eta} \int_0^l dx [P_1(f_{ext} - \partial_x W_1) + P_2(f_{ext} - \partial_x W_2)], \quad (19)$$

where the P_i satisfy the normalization condition

$$\int_0^l dx [P_1 + P_2] = 1. \quad (20)$$

The properties of this two-state models have been discussed in Refs. [4,37,39,40]. Calculating the average velocity v as a function of the externally applied force f_{ext} often leads to a behavior which is roughly approximated by a linear dependence

$$v \simeq v_0(1 - (f_{ext}/f_s)) \quad (21)$$

for many different choices of the potential shapes and the transition rates. Here, v_0 is the spontaneous velocity at zero force $f_{ext} = 0$ and f_s the stalling force, i.e., the force for which the system stops moving. Deviations from this linear behavior mainly occur for forces larger than the stalling force $|f_{ext}| > |f_s|$ or for forces parallel to its natural direction of motion $f_{ext}/f_s < 0$.

The observed force–velocity curves for kinesin motors show an almost linear behavior which can be characterized by v_0 and f_s defined in (21). While $f_s \simeq 5$ pN does not depend much on experimental conditions, the no-load velocity v_0 depends on ATP concentration and attached viscous loads and is of the order of $1 \mu\text{m/s}$ or smaller [41–43].

The orders of magnitude observed for kinesin can be reproduced by the two-state model. Using e.g. a choice of potentials as shown in Fig. 4 with transitions localized at the potential minimum, the stall force is approximatively given by the potential slope. Choosing a potential amplitude of $U \simeq 20k_B T$ which is of the order of the available chemical energy of $\Delta\mu \simeq 15\text{--}20k_B T$ and a period of $l/2 \simeq 8$ nm of microtubules, this force is $f_s \simeq U/l = 5$ pN consistent with the observed value. The spontaneous velocity of the two-state model can be estimated by $v_0 \simeq l/(t_c + t_s)$, where t_c is the time of the chemical steps and $t_s \simeq l^2\eta/U$ is the sliding time in the potential. Therefore, the observation of v_0 alone does not fix both the chemical rate and the value of η corresponding to protein friction. If we assume that for large ATP concentration $t_c \simeq \omega_2^{-1}\Omega^{-1}$ is negligible and the friction η determines the sliding velocity $v_0 \sim U/l\eta$. Using a value of $v_{max} \sim 10^{-5}$ m/s, for the maximal velocity at high ATP concentration, we estimate $\eta \sim 10^{-7}$ which can be seen as an upper bound since chemical steps which, in general, also contribute to friction are neglected. Note that the mechanical properties of a motor depend, in general, both on ATP concentration and of the concentrations of the hydrolysis products [44].

A key parameter characterizing the conditions of operation of the two-state model is the dimensionless value $U/\xi l^2 \Omega \omega_2$ which compares the typical chemical transition time with sliding times in the potential slope. With the arguments given above we estimate $U/\xi l^2 \Omega \omega_2 \simeq 0.1\text{--}1$, where we have used $\Omega \omega_2 \simeq 10^3 \text{ s}^{-1}$ which is a typical transition rate [45]. However, different values are also consistent with the observed force–velocity relation as the spontaneous velocity v_0 is determined by the longest of the two time scales mentioned above. Additional information such as velocity fluctuations would be required to determine this value from experimental observations and to fix the orders of magnitude of all parameters of the model.

The two-state model is consistent with the observed behaviors for biological motor molecules and reproduces typical velocities and forces and the force–velocity relation. Other types of models which use different representations of states and transitions have also been used to consistently describe the force–velocity relation of kinesin [3,27,34–36,46].

5. Energy transduction and efficiency

In the presence of an external force f_{ext} , the system can perform mechanical work, i.e., it operates as a motor. The work performed per unit time against the external force is

$$\mathcal{W} = -f_{ext}v. \quad (22)$$

The chemical energy consumed per unit time is given by

$$\mathcal{Q} = r\Delta\mu. \quad (23)$$

Here, we have introduced the ATP hydrolysis rate r which denotes the number of chemical cycles performed per unit time [4]. Using the rates introduced in Eqs. (10) and (11),

$$r = \int_0^l dx[\alpha_1 P_1 - \alpha_2 P_2] = \int_0^l dx[\beta_2 P_2 - \beta_1 P_1]. \quad (24)$$

We can therefore define the efficiency of energy transduction

$$\eta = -\frac{f_{ext}v}{r\Delta\mu}. \quad (25)$$

This quantity is useful for forces applied opposite to the direction of motion where $0 \leq \eta \leq 1$. Note that this definition relies on the fact that a bulk solution exists which plays the role of a thermodynamic reservoir and allows to define the chemical potentials of fuel and products. In practical situations, the reservoirs may be small and not in local equilibrium. In such a case the efficiency would be more difficult to define.

If $\Delta\mu = 0$, the transition rates defined by Eq. (15) satisfy

$$\omega_1/\omega_2 = e^{-\Delta W/k_B T}, \quad (26)$$

where

$$\Delta W(x) = W_2(x) - W_1(x). \quad (27)$$

The condition of detailed balance for the total transition rates indicates that transitions are just thermal fluctuations and that the system is not driven chemically. If the external force also vanishes, the steady state is a thermal equilibrium with $P_i = Ne^{-W_i(x)/k_B T}$ for which $v = 0$ and $r = 0$. For $\Delta\mu > 0$, the system is chemically driven. If no external force is applied spontaneous motion with $v \neq 0$ can occur, however, only if the system is polar. For a symmetric system with $W_i(x) = W_i(-x)$ and $\omega_i(x) = \omega_i(-x)$ the steady state distributions are also symmetric $P_i(x) = P_i(-x)$. Since $\partial_x W_i$ is antisymmetric in this case, $v = 0$ by symmetry according to Eq. (19). On the other hand, r is, in general, nonzero in this case (the functions α_i are symmetric). For spontaneous motion to occur two requirements have to be fulfilled: detailed balance of the transition has to be broken, which corresponds to $\Delta\mu \neq 0$ and the system must have polar symmetry. In the case of motor proteins the filament polarity plays this role.

For a discussion of physical aspects of motion, it is useful to write

$$\omega_1(x) = \omega_2(x)(\Omega(x) + e^{-\Delta W/k_B T}), \quad (28)$$

where

$$\Omega(x) = e^{-\Delta W/k_B T}(e^{\Delta\mu/k_B T} - 1)\alpha/(\alpha + \beta) \quad (29)$$

which characterizes locally the rate of those transitions which violate detailed balance. Using the dependence of the chemical potential on particle concentration, $\mu_i = \mu_i^0 + k_B T \ln C_i$, we observe that

$$\Omega \sim \left(\frac{C_{ATP}}{C_{ADP}C_P} - k^0 \right), \quad (30)$$

where $k^0 = e^{(\mu_{ATP}^0 - \mu_{ADP}^0 - \mu_P^0)/k_B T}$ is the equilibrium constant of the hydrolysis reaction. Ω therefore is a direct measure of the distance from chemical equilibrium. From Eqs. (29) and (30) we find

$$\Omega \sim \begin{cases} \Delta\mu & \text{for } \Delta\mu/k_B T \ll 1, \\ C_{ATP}/C_{ADP}C_P & \text{for } \Delta\mu/k_B T \gg 1. \end{cases} \quad (31)$$

For our discussion of the two-state model it is useful to characterize the system by the functions ω_2 and Ω instead of α and β which allows us to discuss motion generation without the need to introduce chemistry. This choice is more general and can be used also for cases where transitions between states are triggered by other processes than chemistry such as in artificially constructed systems [47–49].

6. Cooperative action of motors and collective effects

In many interesting situations, a large number of motor molecules operate collectively. Generalizing the simple two-state model to situations where many motors are coupled rigidly, new types of behaviors of the system can occur. This situation can be described by a simple two-state model for the probability density $P_i(\xi, t)$ to find a motor at position ξ in state $i = 1, 2$, which is normalized to $P_1 + P_2 = \ell^{-1}$. It satisfies the dynamic equations

$$\begin{aligned}\partial_t P_1 &= -v\partial_\xi P_1 - \omega_1 P_1 + \omega_2 P_2, \\ \partial_t P_2 &= -v\partial_\xi P_2 + \omega_1 P_1 - \omega_2 P_2,\end{aligned}\tag{32}$$

where the convective terms $v\partial_\xi P_i$ describes rigidly coupled motors. Again, ω_1 and ω_2 are the rates of chemical transition between the two conformations of the motors. The velocity $v = \lambda^{-1}(f_{ext} + f_{mot})$ is generated by the sum of the externally applied force per motor f_{ext} and the average force

$$f_{mot} = - \int_0^\ell d\xi (P_1 \partial_\xi W_1 + P_2 \partial_\xi W_2)\tag{33}$$

generated per motor. The friction coefficient per motor is denoted as λ . If the transition rates $\omega_i(\xi)$ are localized in the potential minima, a dynamic instability in the force–velocity curve appears beyond a critical value of the transition rates [4,50] see Fig. 5. Such a dynamic instability resembles a first order phase transition and implies that in a certain range of forces two distinct stationary states are stable with different velocities.

An interesting result is that even if the potentials are symmetric, motion can occur via spontaneous symmetry breaking. In this case, two spontaneously moving states with opposite velocities coexist in the absence of external forces. In practice, this dynamic symmetry breaking transition is concealed by noise. If the number of collectively operating motors is finite, they generate fluctuations which induce transitions between the two oppositely moving states. As a consequence, the system exhibits bidirectional motion where it moves a certain time in one direction before it switches stochastically to motion in the opposite direction.

Recently, such bidirectional motion has been observed in the so-called motility assays [51]. Motor molecules are attached to a glass surface at high density and in the presence of ATP drive the motion of microtubules which adhere to the motor-coated substrate. Usually, the generated motion occurs with one particular end of the microtubule in front as the microtubule is moved by forces generated towards one end. For a particular mutant of a kinesin motor, the observed behavior is significantly different. It was observed that microtubules switched their direction of motion after times of several seconds up to a minute and the overall motion is bidirectional. At the same time, individual motors of this type are not able to generate motion. This suggests that the individual motors have lost their directionality as a result of the mutation. At the same time, collections of these motors are still able to generate motion via a symmetry breaking dynamic instability. We have shown that this interpretation provides a natural explanation of the experimental observations [52]. Interesting collective effects can also occur due to crowding of many motors on a filament along which they advance [53,54].

A natural consequence of a dynamic instability in the force–velocity relationship of a collection of motor proteins is the possibility to generate spontaneous oscillations [14,15]. In the presence of an additional

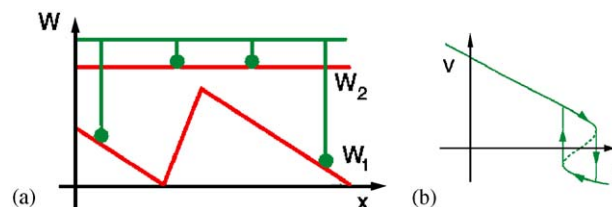


Fig. 5. Collective effects of many motors which interact rigidly. (a) Ratchet model for cooperative motors. For large number of motors this system can exhibit dynamic instabilities in its active mechanical properties. (b) Force–velocity relationship which exhibits a dynamic instability. In a range of forces f , two steady states coexist with different velocity v .

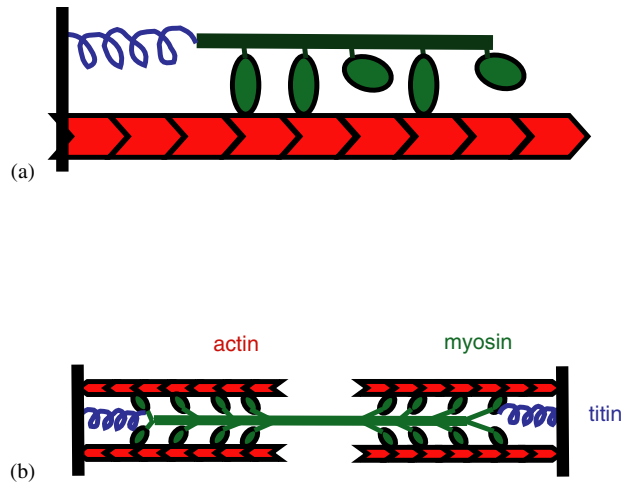


Fig. 6. Collective motors coupled with elastic elements can generate spontaneous oscillations. (a) Motor collection working against an elastic spring. If the motor collection has a dynamic instability in its force–velocity relationship (see Fig. 5), the system can become self-oscillatory. (b) Schematic structure of sarcomeres in muscles. Many myosin motors work on actin filaments. Molecules such as titin represent elastic elements. Muscles therefore, in general, could become unstable with respect to spontaneous oscillations.

elastic element of modulus k against which the motor collection works, the velocity becomes $v = \lambda^{-1}(f_{ext} + f_{mot} - kx)$, see Fig. 6. If the chemical rates are varied, the system can change its behavior from a stationary state without net motion to periodic oscillatory movements. These oscillations emerge at an instability called Hopf bifurcation. Changing the chemical rates to bring the system to an oscillatory regime could be achieved by varying the ATP concentration or alternatively the concentration of regulatory agents such as the concentration of Ca^{++} . The oscillation frequency at the bifurcation point can be estimated as

$$\omega_c \simeq \left(\frac{\alpha k}{\lambda} \right)^{1/2}, \tag{34}$$

where $\alpha = \omega_1 + \omega_2$ is a characteristic rate of the ATP hydrolysis cycle of the motors. If the stiffness k becomes large, frequencies can become high. The highest frequency $\omega_{max} \simeq (\alpha K_{cb}/\lambda)^{1/2}$ the system can attain at the bifurcation is limited by the cross-bridge elasticity K_{cb} and can exceed α . Far from the bifurcation, relaxation oscillations occur where the motor collection switches periodically between two coexisting states with opposite directionality.

Such oscillations are relevant for some cellular systems. Muscles contain large collections of myosin motors. In addition molecules such as titin can play the role of elastic elements (see Fig. 6). Therefore, muscles, in general, can become self-oscillatory. Spontaneous oscillations of ordinary muscles have been observed under un-physiological conditions [55,56]. Some muscles can oscillate spontaneously as a part of their normal function. The flight muscles of many insects which drive the wing-beat spontaneously generate periodic contractions [57]. Collective motor behavior is a general physical mechanism which can explain such behaviors [58].

7. Self-organization of motors and filaments

If motors form small aggregates, they can interact with two or more filaments at the same time. Such aggregates then play the role of cross-linkers of a filament network. Since a motor can move along a given filament, these cross-links are mobile and the resulting polymer network intrinsically dynamic [59–61]. Experimentally, such filament systems in the presence of mobile cross-linkers can be studied using artificial constructs linking motors together. It has been shown that such systems self-organize and generate spatiotemporal patterns such as asters and vortices [7,8,62,63].

A case of particular importance is the situation where filaments are aligned and form a bundle [9–11]. The dynamic and mechanic properties of active bundles can be discussed in very simplified physical models. Using a one-dimensional description of the bundle, we denote by $c^+(x)$ and $c^-(x)$ the densities of filaments pointing their plus ends to the right and left, respectively. Assuming that mobile cross-links induce interactions predominantly of filament pairs, we can write nonlinear dynamic equations for the filament densities. In this description, filament currents are resulting from active behaviors of motors, which induce the relative sliding of filament pairs. The densities obey dynamic equations based on conservation laws:

$$\begin{aligned}\partial_t c^+ &= D\partial_x^2 c^+ - \partial_x J^{++} - \partial_x J^{+-}, \\ \partial_t c^- &= D\partial_x^2 c^- - \partial_x J^{-+} - \partial_x J^{--}.\end{aligned}\quad (35)$$

Here, the diffusion terms with coefficient D result from fluctuations both thermal and nonthermal and the active currents $J^{\pm\pm}$ are induced by motors which slide filaments relative to each other. They can be written as

$$\begin{aligned}J^{\pm\pm}(x) &= \alpha \int_0^\ell d\xi [c^\pm(x + \xi) - c^\pm(x - \xi)]c^\pm(x), \\ J^{\pm\mp}(x) &= \pm\beta \int_{-\ell}^\ell d\xi c^\mp(x + \xi)c^\pm(x),\end{aligned}\quad (36)$$

where ℓ denotes the filament length.

The form of these interaction terms can be obtained from symmetry arguments. We have to distinguish between two types of interactions. Interactions between filaments of equal orientation, characterized by an interaction strength α and interactions between filaments of opposite orientation with strength β . We find that interaction between equally oriented filaments can generate a contractile tension and induces the shortening of a bundle. For sufficiently large values of α , a homogeneous density profile becomes unstable and contracts to become a localized distribution. If furthermore the interaction between oppositely oriented filaments is acting, described by a finite value of β , a dynamic instability again occurs. The homogeneous state now becomes unstable with respect to propagating modes if periodic boundary conditions are imposed. These solitary waves can upon further increase of α turn into more complex oscillating wave patterns.

This simplified description, which is based on basic rules of filament sliding, already leads to a rich scenario of bifurcations and dynamic instabilities. Higher-dimensional systems and highly cross-linked gels with active properties due to the action motor proteins present an additional challenge. Generalized hydrodynamic approaches which take into account active stresses generated by motors as well as the average orientation of polar filaments can capture general features of the material properties and the dynamic of such systems on large scales [12,13].

8. Dynamics of cilia

Complex dynamic patterns generated by the action of motor proteins are used by many microorganisms to swim in a viscous fluid. Cilia and flagella are hair-like appendages of many cells which contain microtubules arranged in a cylindrical geometry together with a large number of dynein motors [1]. These structures of motors and microtubules are called axonemes, see Fig. 7(a). They are able to generate bending waves as a result of motor action which propagate along these long elastic structures.

Bending deformations of the axoneme are induced by internal forces which slide neighboring microtubules relative to each other. If global sliding is blocked by a rigid connection between microtubules at one end, the system bends in response to sliding. Mechanical oscillations occur if the system undergoes an oscillating instability or Hopf bifurcation. Collectively operating motors can undergo in such a geometry an oscillating instabilities which lead to bending waves [16,64]. This is a generalization of the spontaneous oscillations of a motor collection which works against an elastic element described above. In the case of the axoneme, it is the bending elasticity of the microtubules which plays the role of an elastic spring. The bending deformations induced by the motors lead to the generation of bending waves. In the vicinity of a Hopf bifurcation, the linearly unstable bending waves are solutions to the linear wave equation. For planar

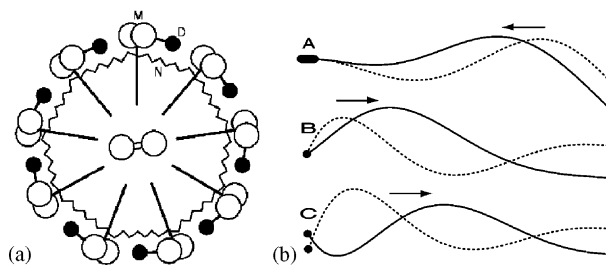


Fig. 7. (a) Schematic cross-section of an axoneme which is the motile element in cilia and eucaryotic flagella. Nine doublets of microtubules are arranged in a cylindrical geometry. A central pair of microtubules is located in the center. Dynein motor proteins are attached in large numbers on the outer microtubules and exert forces on neighboring microtubules. (b) Bendin wave patterns of an active cilium calculated near an oscillating instability for different boundary conditions at the head. (A—clamped head, B—pivoting head, C—free head with viscous load corresponding to a swimming sperm.) The arrows indicate the direction of wave propagation (from Ref. [16]).

waves it reads

$$-i\omega\xi\tilde{\psi} = -\kappa\partial_s^4\tilde{\psi} + a^2\chi\partial_s^2\tilde{\psi}. \tag{37}$$

Here, the shape of the cilium is described by the local angle $\psi(s, t) = \tilde{\psi}(s)e^{-i\omega t} + \text{c.c.}$ of the cilium with respect to the beat axis, s is the arclength along the cilium and ω the angular frequency of the beat. The total bending rigidity of all the microtubules in the axoneme is denoted as κ and ξ denotes the coefficient of hydrodynamic friction per unit length. The active properties of the collection of motors together with passive linkers between the microtubule doublets inside the cilium are described by the linear response function $\chi(\omega)$ which is complex valued. These planar waveforms can be calculated if boundary conditions are specified, see Fig. 7. Indeed, many simple waves such as for example the waves generated by many sperm to swim are planar and can be compared.

9. Mechanosensory cells and critical oscillators

In the previous sections, we have demonstrated that cytoskeletal structures which contain motor molecules can exhibit rich dynamic behaviors and can undergo dynamic instabilities. Such phenomena are also relevant for mechanosensory cells of the inner ears of vertebrates where oscillatory instabilities and spontaneous oscillations play an important role [17,18,20,65]. Hair cells are specialized sensory cells which possess at their surface a bundle of rod-like structures mainly formed by densely packed actin filaments. This hair bundle is a mechano-electrical transducer, capable of detecting bundle deflections of a few nm and generating an electrical membrane potential in response [19].

It has been shown recently that hair bundles in frog ears exhibit spontaneous oscillatory motion [20,66–68]. It has been shown that these spontaneous movements are the signature of an active process which can amplify periodic mechanical stimuli in a frequency selective way. If the hair bundle is stimulated by a periodic force $f(t) = \tilde{f}e^{-i\omega t} + \text{c.c.}$, the sensitivity $|\tilde{x}|/|\tilde{f}|$ of the oscillating hair bundle increases for small stimuli if the stimulus frequency is in the vicinity of the spontaneous frequency of oscillation of the cell [66]. Here, \tilde{x} is the phase locked Fourier amplitude of the response.

This signal amplification can be understood if we assume that the hair bundle profits from the nonlinear properties of an oscillator in the vicinity of a Hopf bifurcation [17,18]. A nonlinear mechanical oscillator has general properties. At a Hopf bifurcation, the mode $\tilde{x} = x_1$ with angular frequency ω becomes unstable. Nonlinearities lead to the generation of higher harmonics x_n with $|n| > 1$. The spontaneous oscillation therefore corresponds to a displacement $x(t) = \sum_n x_n e^{-i\omega t}$. The instability of the fundamental mode can be captured by the general expansion

$$\tilde{f} = A\tilde{x} + B|\tilde{x}|^2\tilde{x} + O(|\tilde{x}|^4\tilde{x}), \tag{38}$$

where $A = \chi(\omega)^{-1}$ is a linear response coefficient introduced in the last section and B is a complex coefficient which describes the dominant nonlinearity. We assume that the behavior of the system can be changed from

quiescent to spontaneous oscillations by varying a control parameter C . In the absence of a stimulus, $\tilde{f} = 0$, and the amplitude of the unstable mode is given by

$$|\tilde{x}|^2 = -\frac{A}{B}. \quad (39)$$

The Hopf bifurcation occurs at a critical value $C = C_c$ and generates oscillations with frequency ω_c . It is characterized by the condition that $A(C_c, \omega_c) = 0$. Close to the bifurcation we can therefore express this coefficient by a systematic expansion of the form

$$\mathcal{A}(\omega, C) \simeq \alpha(\omega - \omega_c) + \beta(C - C_c). \quad (40)$$

As a consequence, if the system is operating at the critical point $C = C_c$, $A \sim (\omega - \omega_c)$ vanishes at the characteristic frequency. If the system is stimulated at this frequency, the linear term vanishes and the response is

$$|\tilde{x}| \sim |\tilde{f}|^{1/\delta} \quad (41)$$

with $\delta = 3$. Consequently the sensitivity of the system $|\tilde{x}|/|\tilde{f}| \sim f^{-2/3}$ becomes large for small stimulus amplitudes. This compressive nonlinear response is ideally suited for frequency selective vibration detection over a large dynamic range. With our ears we can detect sound over six orders of magnitude of sound pressure. This requires a compressive nonlinear response to be possible as the range of vibration amplitudes of highly sensitive mechanosensors is limited. Assuming a compressive nonlinear response of mechanosensors with $\delta = 3$ this corresponds to a range of vibration amplitudes of only two orders of magnitudes in the ear, which is in the physiologically permissive range.

A Hopf bifurcation of a complex nonlinear dynamic system which consists of a large number of coupled degrees of freedom can be related to critical points in extended thermodynamic systems [69,70]. Consider a large number of noisy, oscillating variables which are arranged on a d -dimensional lattice and coupled to their neighbors. Such a system undergoes beyond a critical coupling strength a sharp synchronization transition in a thermodynamic limit. At this transition, spontaneous oscillations emerge which are coherent over long times. This transition is a nonequilibrium critical point with universal properties. In general, the critical exponent δ depends on the space dimension. Above the upper critical dimension $d = 4$, mean field theory applies which is described by Eq. (38) and for which $\delta = 3$. This relation of Hopf bifurcations to the concepts of universality and critical points assures that frequency selectivity and the compressive nonlinear response required for hearing is reliably achieved in the ears of vertebrate animals, even though the underlying cellular structures and microscopic mechanisms for oscillation generation can differ significantly. An important question which remains is how dynamic oscillators in the ear could reliably achieve proximity to a critical point. It has been suggested that a general self-regulation mechanism could bring the system close to the critical point by a feedback control [17].

10. Outlook

We have seen in the previous sections that many complex dynamic cellular processes in eucaryotic cells result from the interplay of large numbers of proteins in the cytoskeleton. These processes take place in the cell at roughly constant temperature but far from thermodynamic equilibrium and are driven by metabolic chemical energy such as the hydrolysis of ATP. In this situation, the self-organization of the components leads to the emergence of collective modes which undergo complex spatiotemporal dynamics. Important examples are oscillations and wave-like modes and the active properties of inherently active materials. In addition, the stochastic nature of molecular processes leads to fluctuations which play an important role because of the small scale of cells. The physical description of cellular force generation therefore combines concepts from statistical physics and nonlinear dynamics.

In the cell, such dynamic phenomena are tightly controlled and related to cellular functions. In particular, cell division requires an intricate sequence of complex, pattern forming, dynamic events. The reliability of cell division which is essential for the survival of the cell is achieved by the so-called check-points. At these check-points, criteria have to be met before the cell continues its cellular cycle of division.

The self-organization phenomena and the statistical physics of cellular force generation described here can be studied in *in vitro* assays where purified components are mixed in a test tube. This provides insight in the dynamics resulting from the interplay of certain molecules. In the future, it will be important to bring together studies of the control and regulatory systems of the cell with the statistical physics and biophysics of force generation. This could allow us to move towards a theoretical understanding of cellular functions and could stimulate closer interactions of cell biology and cellular biophysics. We expect that this will open a role for theoretical and quantitative methods in cell biology.

Acknowledgments

I thank T. Bollenbach, M. Betterton, S. Camalet, M. Dogterom, T. Duke, M. Cosentino-Lagomarsino, S. Grill, J.-F. Joanny, A. Hilfinger, J. Howard, G. Klein, K. Kruse, B. Nadrowski, P. Martin, B. Mulder, J. Prost, I. Rcidel-Kruse, T. Risler, K. Sekimoto, C. Tanase and A. Zumdieck for stimulating collaborations.

References

- [1] D. Bray, *Cell Movements*, Garland Publishing, New York, 2001.
- [2] B. Alberts, et al., *Molecular Biology of the Cell*, Garland Science, New York, 2002.
- [3] J. Howard, *Mechanics of Motor Proteins and the Cytoskeleton*, Sinauer Associates Inc., Sunderland, 2001.
- [4] F. Jülicher, A. Ajdari, J. Prost, *Rev. Mod. Phys.* 69 (1997) 1269.
- [5] R.D. Astumian, *Science* 276 (1997) 917.
- [6] K. Takiguchi, *J. Biochem.* 109 (1991) 502.
- [7] F.J. Nédélec, T. Surrey, A.C. Maggs, S. Leibler, *Nature* 389 (1997) 305.
- [8] T. Surrey, M.B. Elowitz, P.-E. Wolf, F. Yang, F. Nédélec, K. Shokat, S. Leibler, *J. Proc. Natl. Acad. Sci. USA* 95 (1998) 4293.
- [9] K. Kruse, F. Jülicher, *Phys. Rev. Lett.* 85 (2000) 1778.
- [10] K. Kruse, S. Camalet, F. Jülicher, *Phys. Rev. Lett.* 87 (2001) 138101-1.
- [11] K. Kruse, F. Jülicher, *Phys. Rev. E* 67 (2003) 051913.
- [12] K. Kruse, J.F. Joanny, F. Jülicher, J. Prost, K. Sekimoto, *Phys. Rev. Lett* 92 (2004) 078101.
- [13] K. Kruse, J.F. Joanny, F. Jülicher, J. Prost, K. Sekimoto, *Eur. Phys. J. E* 16 (2005) 5.
- [14] F. Jülicher, J. Prost, *Phys. Rev. Lett.* 78 (1997) 4510.
- [15] S. Grill, K. Kruse, F. Jülicher, *Phys. Rev. Lett.* 94 (2005) 108104.
- [16] S. Camalet, F. Jülicher, *New J. Phys.* 2 (2000) 24.
- [17] S. Camalet, T. Duke, F. Jülicher, J. Prost, *Proc. Natl. Acad. Sci. USA* 97 (2000) 3183.
- [18] V.M. Eguiluz, M. Ospeck, Y. Choe, A.J. Hudspeth, M.O. Magnasco, *Phys. Rev. Lett.* 84 (2000) 5232.
- [19] A.J. Hudspeth, *Curr. Opin. Neurobiol.* 7 (1997) 480.
- [20] P. Martin, A.J. Hudspeth, *Proc. Natl. Acad. Sci. USA* 96 (1999) 14306.
- [21] P. Martin, A.D. Metha, A.J. Hudspeth, *Proc. Natl. Acad. Sci. USA* 97 (2000) 12026.
- [22] B. Nadrowski, P. Martin, F. Jülicher, *Proc. Natl. Acad. Sci.* 101 (2004) 12195.
- [23] A.F. Huxley, *Prog. Biophys.* 7 (1957) 255.
- [24] A.F. Huxley, B. Simmons, *Nature* 233 (1971) 533.
- [25] T.L. Hill, *Prog. Biophys. Mol. Biol.* 28 (1974) 267.
- [26] J.A. Spudich, *Nature (London)* 348 (1990) 284.
- [27] C.S. Peskin, G.B. Ermentrout, G.F. Oster, in: V. Mow, et al. (Eds.), *Cell Mechanics and Cellular Engineering*, Springer, New York, 1994.
- [28] J. Prost, J.F. Chauwin, L. Peliti, A. Ajdari, *Phys. Rev. Lett.* 72 (1994) 2652.
- [29] R.D. Astumian, M. Bier, *Phys. Rev. Lett.* 72 (1994) 1766.
- [30] P. Reimann, *Phys. Rep.* 361 (2002) 57.
- [31] R.P. Feynman, R.B. Leighton, M. Sands, *The Feynman Lectures on Physics*, vol. I, Addison-Wesley, Reading, MA, 1966 (Chapter 46).
- [32] H. Risken, *The Fokker–Planck Equation*, Springer, Berlin, 1984.
- [33] S. Leibler, D. Huse, *J. Cell Biol.* 121 (1993) 1357.
- [34] T. Duke, S. Leibler, *Biophys. J.* 71 (1996) 1235.
- [35] A.B. Kolomeisky, M.E. Fisher, *J. Chem. Phys.* 113 (2000) 10667.
- [36] M.E. Fisher, A.B. Kolomeisky, *Proc. Natl. Acad. Sci. USA* 98 (2001) 7748–7753.
- [37] A. Ajdari, *J. Prost, C.R. Acad. Sci. Paris II* 315 (1992) 1635.
- [38] S.M. Block, *J. Cell Biol.* 140 (1998) 1281.
- [39] J.F. Chauwin, A. Ajdari, J. Prost, *Europhys. Lett.* 27 (1994) 421.
- [40] J.F. Chauwin, A. Ajdari, J. Prost, *Europhys. Lett.* 32 (1995) 373.

- [41] K. Svoboda, S. Block, *Cell* 77 (1994) 773.
- [42] A.J. Hunt, F. Gittes, J. Howard, *Biophys. J.* 67 (1994) 766.
- [43] E. Mayhofer, J. Howard, *Proc. Natl. Acad. Sci.* 92 (1995) 574.
- [44] W.R. Schief, R.H. Clark, A.H. Crevenna, J. Howard, *Proc. Natl. Acad. Sci.* 101 (2004) 1183.
- [45] S.P. Gilbert, M.R. Webb, M. Brune, K.A. Johnson, *Nature* 373 (1995) 671.
- [46] I. Derényi, T. Vicsek, *Proc. Natl. Acad. Sci.* 93 (1996) 6775.
- [47] J. Rousset, L. Salome, A. Ajdari, J. Prost, *Nature* 370 (1994) 446.
- [48] L.P. Faucheux, A. Libchaber, *J. Chem. Soc. Faraday Trans.* 91 (1995) 3163.
- [49] L. Gorre, E. Ioannidis, P. Silberzan, *Europhys. Lett.* 33 (1996) 267.
- [50] F. Jülicher, J. Prost, *Phys. Rev. Lett.* 75 (1995) 2618.
- [51] S.A. Endow, H. Higuchi, *Nature (London)* 406 (2000) 913.
- [52] M. Badoual, F. Jülicher, J. Prost, *Proc. Natl. Acad. Sci. USA* 99 (2002) 6696.
- [53] K. Kruse, K. Sekimoto, *Phys. Rev. E* 66 (2002) 031904.
- [54] A. Parmeggiani, T. Franosch, E. Frey, *Phys. Rev. Lett.* 90 (2003) 086601.
- [55] K. Yasuda, Y. Shindo, S. Ishiwata, *Biophys. J.* 70 (1996) 1823.
- [56] H. Fujita, S. Ishiwata, *Biophys. J.* 75 (1998) 1439.
- [57] J.W.S. Pringle, in: R.T. Tregear (Ed.), *Insect Flight Muscle*, North-Holland, Amsterdam, 1977, p. 177.
- [58] F. Jülicher, J. Prost, *Phys. Rev. Lett.* 83 (1999) 5404.
- [59] T. Liverpool, A.C. Maggs, A. Ajdari, *Phys. Rev. Lett.* 86 (2001) 4171.
- [60] L. LeGoff, F. Amblard, E.M. Furst, *Phys. Rev. Lett.* 88 (2002) 018101.
- [61] D. Humphrey, C. Duggan, D. Saha, D. Smith, J. Käs, *Nature* 416 (2002) 744.
- [62] F.J. Nédélec, T. Surrey, A.C. Maggs, *Phys. Rev. Lett.* 86 (2001) 3192.
- [63] H.Y. Lee, M. Kardar, *Phys. Rev. E* 64 (2001) 056113.
- [64] S. Camalet, F. Jülicher, J. Prost, *Phys. Rev. Lett.* 82 (1999) 1590.
- [65] Y. Choe, M.O. Magnasco, A.J. Hudspeth, *Proc. Natl. Acad. Sci. USA* 95 (1998) 15321.
- [66] P. Martin, A.J. Hudspeth, *Proc. Natl. Acad. Sci. USA* 98 (2001) 14386.
- [67] R. Fettiplace, A.J. Ricci, C.M. Hackney, *Trends Neurosci.* 24 (2001) 169.
- [68] P. Martin, J.A. Hudspeth, F. Jülicher, *Proc. Natl. Acad. Sci. USA* 98 (2001) 14380.
- [69] T. Risler, J. Prost, F. Jülicher, *Phys. Rev. Lett.* 93 (2005) 175702.
- [70] T. Risler, J. Prost, F. Jülicher, *Phys. Rev. E* 72 (2005) 06130.